the module block to achieve high reliability. High optical responsivity including a coupling efficiency of 0.84A/W was obtained at 1.55μm. The electrical signal from the distributed amplifier IC was guided by a ceramic coplanar waveguide, and was output through a V-connector. The optical signal frequency response is shown in Fig. 4. The 3dB bandwidth was 41GHz, which is limited by the distributed amplifier IC. Gain ripple was < 1.5dB.

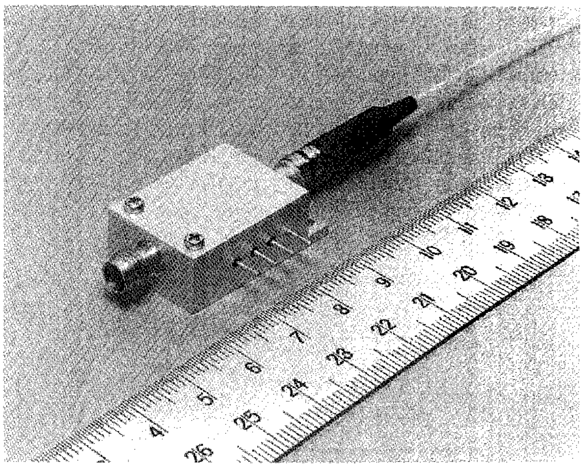

Fig. 3 *Photograph of receiver module*

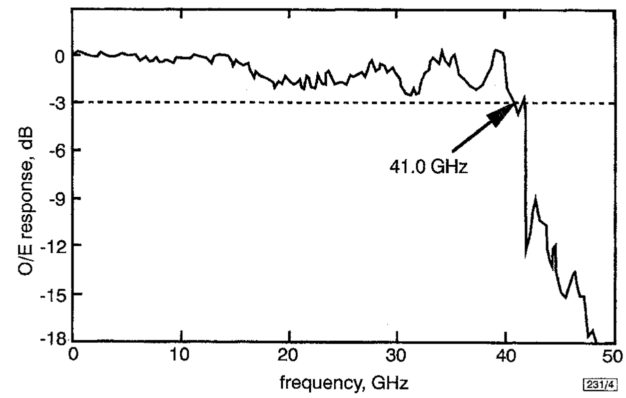

Fig. 4 *Frequency response*

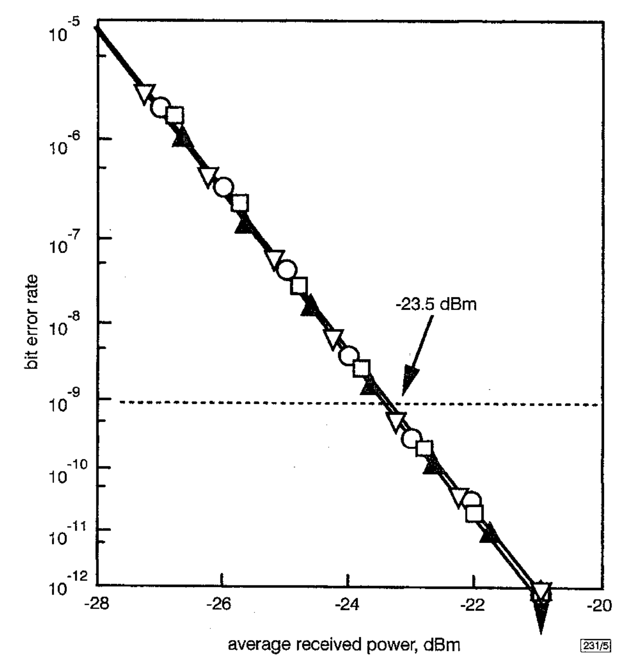

Fig. 5 *Bit error rate characteristics*

40Gbit/s RZ
□ 10 Gbit/s channel 1
▽ 10Gbit/s channel 2
▲ 10Gbit/s channel 3
○ 10Gbit/s channel 4

40Gbit/s receiver sensitivity measurements: Receiver sensitivity was measured at 40Gbit/s. Four pairs of 10Gbit/s NRZ data signals (pattern length: 2^7–1) were electrically multiplexed to generate 40Gbit/s NRZ signals by InP HEMT ICs [5]. 40GHz short optical pulse trains from a mode-locked LD module were externally modulated by an LN Mach-Zehnder modulator driven by the amplified 40Gbit/s NRZ signals. The pulse width was 5ps (FWHM). The bit error rate was checked for all four-channel electrically demultiplexed 10Gbit/s signals. As shown in Fig. 5, the receiver sensitivity of the worst 10 Gbit/s channel was –23.5dBm at a bit error rate of 10^{-9} with an EDFA preamplifier (NF: 5.0dB). The receiver sensitivity difference was < 0.2dB and there was no error floor.

Conclusion: A 41GHz baseband optical receiver has been constructed by using flip-chip bonding between a WGPD and a GaAs-MESFET baseband-type distributed amplifier IC. An impedance-matching interconnection line between those two devices was designed. The receiver sensitivity measurement confirms the application of this module to 40Gbit/s optical receivers.

5 January 1998
Electronics Letters Online No: 19980337

Y. Miyamoto and M. Yoneyama, (*NTT Optical Network Systems Laboratories, (Y-808A) 1-1, Hikari-no-oka, Yokosuka-shi, Kanagawa, 239 Japan*)

Y. Imai (*NTT System Electronics Laboratories, (Y-808A) 1-1, Hikari-no-oka, Yokosuka-shi, Kanagawa, 239 Japan*)

K. Kato and H. Tsunetsugu (*NTT Opto-electronics Laboratories, (Y-808A) 1-1, Hikari-no-oka, Yokosuka-shi, Kanagawa, 239 Japan*)

E-mail: miyamoto@exa.onlab.ntt.co.jp

References

1 TSUDA, H., MIYAMOTO, Y., SANO, A., KATO, K., IMAI, Y., and HAGIMOTO, K.: '40Gbit/s baseband-type optical receiver module using a waveguide photodetector and a GaAs MESFET distributed amplifier IC'. OECC'97 Tech. Dig., 1996, Paper 19A1-2, pp. 506–507

2 KIMURA, S., and IMAI, Y.: 'DC-to-40GHz GaAs MESFET distributed baseband amplifier IC'. APMC'94 Tech. Dig., 1994, Vol. 1, pp. 249–252

3 KATO, K., HATA, S., KUWANO, K., YOSHIDA, J., and KOZEN, A.: 'A high-efficiency 50GHz InGaAs multimode waveguide photodetector', *J. Quantum. Electron.*, 1992, **28**, pp. 2728–2735

4 TSUNETSUGU, H., HAYASHI, T., HOSOYA, M., and KATSURA, K.: 'New flip-chip bonding technique using transferred microsolder bumps'. 1st IEMT/IMC Symp., 1997, pp. 56–61

5 YONEYAMA, M., SANO, A., HAGIMOTO, K., OTSUJI, T., MURATA, K., IMAI, Y., YAMAGUCHI, S., ENOKI, T., and SANO, E.: 'A 40Gbit/s optical receiver circuit using InAlAs/InGaAs HEMT Digital IC chip set'. Paper WE1D-2, MTT-S'97 Tech. Dig., 1997, pp. 461–462

Dynamic response of high-speed wavelength selector using hybrid integrated four-channel SS-SOA gate array on PLC platform

T. Ito, I. Ogawa, N. Yoshimoto, K. Magari, F. Ebisawa, Y. Yamada, Y. Yoshikuni and Y. Hasumi

The dynamic response of a high-speed wavelength selector using a fully packaged four-channel semiconductor optical amplifier gate array on a PLC platform is reported. Ultra-wideband (1530–1600nm) operation was successfully demonstrated. The gating time was sufficiently fast at 1ns. The electrical interference between the channels was negligible.

Introduction: The high-speed wavelength selector, the key component of near-future optical network systems [1], will be developed using arrayed waveguide grating (AWG) and optical gate elements. The multi-channel semiconductor optical amplifier (SOA) [2, 3] gate array is one of the most promising candidates for such a gate element because it provides fibre-to-fibre loss-less operation with a high extinction ratio over a wide wavelength range.

Zirngibl *et al.* demonstrated a monolithic integrated wavelength selector with ribloading InGaAsP AWGs and quantum well SOAs [4]. However, it was hard to use in a practical system because it was difficult to achieve polarisation-independence, to drive all SOAs at a high speed of < 1 ns, and to fabricate a large scale gate array.

An effective method for developing a wavelength selector is to use a silica-based planar-lightwave-circuit (PLC) AWG and spot size-converted SOA gate array [5] on a PLC platform. In this Letter, we describe a four-channel wavelength selector using the SS-SOA gate array module and PLC-AWG. Ultra-wideband (1530–1600nm) operation was successfully demonstrated. The gating time was sufficiently fast at 1 ns; electrical interference between the channels was negligible.

SS-SOA gate array on PLC platform: The SS-SOA gate chip [5] consisted of a 600μm bulk active region and two 300μm SS tapered bulk passive regions. The thickness of the active region was 0.4μm. A 0.6μm wide mesa stripe was formed by CH_4/H_2 dry-etching and was buried by the buffer-inserted buried hetero-structure method [6]. After anti-reflection coating, the SS-SOA gate array was bonded with AuSn solder on a PLC platform using passive alignment. Singlemode fibre arrays were butted for both facets of the four-channel silica waveguides.

Fig. 1 shows the wavelength dependence of the extinction ratio and the loss-less current of the module. The extinction ratio was > 35dB and the fibre-to-fibre loss-less current was < 50mA over a wide wavelength range from 1530 to 1600nm. The minimum loss-less current was 25mA for 1580nm.

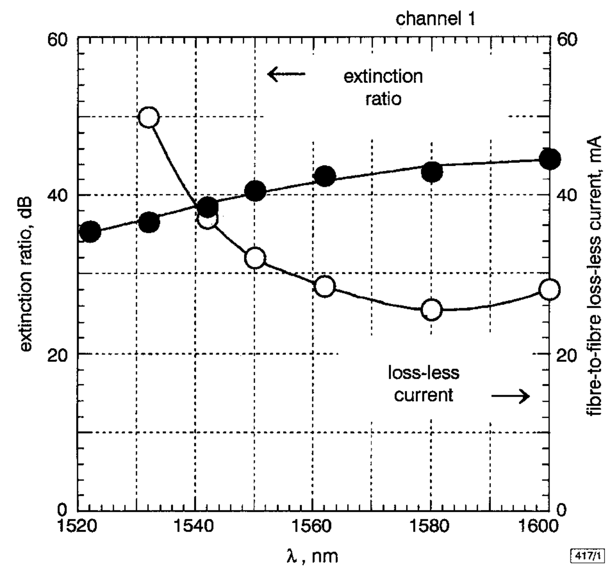

Fig. 1 *Wavelength dependence of SS-SOA gate on PLC platform*

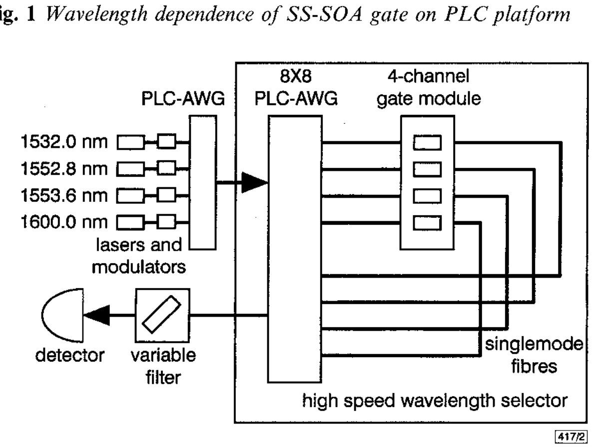

Fig. 2 *Experimental setup of wavelength selector*

Experimental setup: The experimental setup of the wavelength selector is shown in Fig. 2. Four lasers operating at 1532.0, 1553.5, 1554.3 and 1600.0nm, four pulse pattern generators (PPG) and four modulators were used to generate four non-return-to-zero (NRZ) optical signals. The bit rates of the four wavelengths were 2.5, 10, 10 and 622Mbit/s, respectively. The four signals were wavelength multiplexed by a PLC-AWG and were launched into the wavelength selector. The wavelength selector consisted of an 8 × 8 PLC-AWG and a four-channel SOA gate module. The input signals were demultiplexed by the 8 × 8 PLC-AWG and were selected by the SOA gate array. Fibre amplifiers were used to compensate the loss of the PLC-AWGs and modulators, and the optical power of the four signals was –10dBm before the SOA gate array. After the gate array, the four signals were multiplexed again with the 8 × 8 PLC-AWG. A variable optical filter with a bandwidth of 1nm was placed before the O/E receiver. The eye pattern and bit error rate (BER) were measured for each channel.

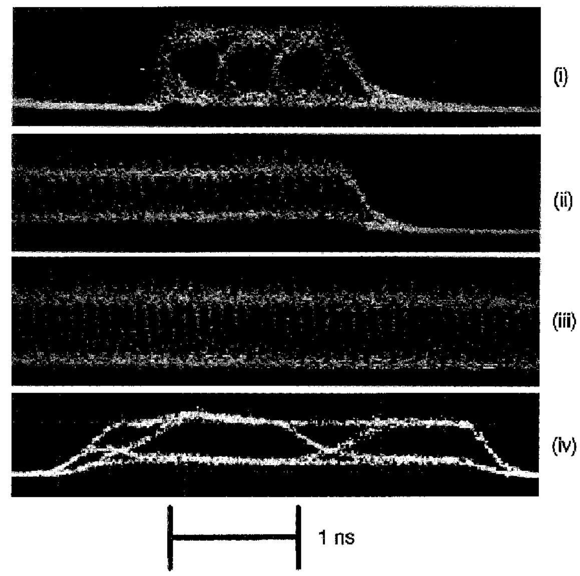

Fig. 3 *Dynamic response of wavelength selector*

(i) channel 1; 1532.0nm, 2.5Gbit/s
(ii) channel 2; 1553.5nm, 10Gbit/s
(iii) channel 3; 1554.3nm, 10Gbit/s
(iv) channel 4; 1600.0nm, 622Mbit/s

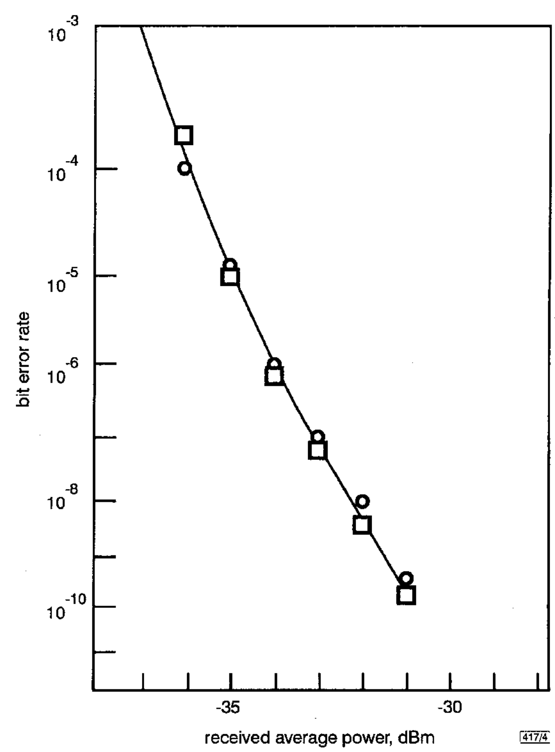

Fig. 4 *Bit error rate of wavelength selector*

□ only channel-3
O channel-3 (all four channels driven)
1554.3nm, –10dBm, 10Gbit/s, NRZ $2^{31}-1$, channel-3, 32mA

Experimental results: Fig. 3 shows the response of the high-speed wavelength selector. It should be noted that the wavelength selector operated over an ultra-wideband from 1532 to 1600nm. Wavelength separation can be set at 0.8nm, as shown as the separation between channels -2 and -3, due to the characteristics of the 8 × 8 PLC-AWG. Both the rise and fall time were < 1 ns, which is suitable for optical packet switching including photonic ATM [1].

Fig. 4 shows the BER of channel-3. The BER was $< 10^{-9}$ at a received averaged power of –31dBm. We carried out the same measurement for the cases when the other channels (-1, -2 and -4) were not driven (□), and for when the other channels were randomly driven (○), as in Fig. 3. No power penalty was observed even when the other channels were randomly driven. The interference between channels was therefore negligible.

Conclusion: The four-channel ultra-wideband (1530–1600nm) wavelength selector was successfully demonstrated. It consisted of a fully packaged four-channel semiconductor optical amplifier gate array on a PLC platform and a PLC-AWG. Ultra-wideband (1530–1600nm) operation was successfully demonstrated. The gating time was sufficiently fast at 1ns; the electrical interference between channels was negligible.

 13 January 1998
Electronics Letters Online No: 19980360

T. Ito, I. Ogawa, N. Yoshimoto, K. Magari, F. Ebisawa, Y. Yamada, Y. Yoshikuni and Y. Hasumi (*NTT Opto-electronics Laboratories, 3-1, Morinosato Wakamiya, Atsugi-shi, Kanagawa Pref., 240-01 Japan*)

E-mail: toshio@aecl.ntt.co.jp

References

1 HABARA, K., YAMADA, Y., MISAWA, A., SASAYAMA, K., TSUKADA, M., MATSUNAGA, T., and YUKIMATSU, K.: 'Demonstration of frequency-routing type photonic ATM switch (FRONTIERNET) prototype'. ECOC'96, Proc., Oslo, Norway, September 1996, Vol. 5, Post-Deadline Paper ThC. 3.4, 5.41

2 LECLERC, D., BROSSON, P., POMMEREAU, F., NGO, R., DOUSSIERE, P., MALLECOT, F., GAVIGNET, P., WAMSLER, I., LAUBE, G., HUNZIKER, W., VOGT, W., and MELCHIOR, H.: 'High-performance semiconductor optical amplifier for self-aligned packaging using Si V-groove flip-chip technique', *IEEE Photonics Technol. Lett.*, 1995, **7**, (5) pp. 476–478

3 GUSTAVSSON, M., LAGERSTORM, B., THYLEN, L., JANSON, M., LUNDGREN, L., MORNER, A.C., RASK, M., and STOLTZ, B.: 'Monolithically integrated 4 × 4 InGaAsP/InP laser amplifier gate switch array', *Electron. Lett.*, 1992, **28**, pp. 2223–2225

4 ZIRNGIBL, M., JOYNER, C.H., and GLANCE, B.: 'Digitally tunable channel dropping filter/equalizer based on waveguide grating router and optical amplifier integration', *IEEE Photonics Technol. Lett.*, 1994, **6**, pp. 513–515

5 YOSHIMOTO, N., MAGARI, K., KAWAGUCHI, Y., KISHI, K., MITOMI, O., KONDO, Y., KADOTA, Y., ITO, T., TOHMORI, Y., YOSHIKUNI, Y., NAKAJIMA, O., and HASUMI, Y.: '4-channel polarization-insensitive semiconductor optical amplifier (SOA) gate array integrated with spot-size converters'. OAA'97, Victoria, Canada, July 1997, Post-deadline paper PD–6

6 KONDO, Y., KISHI, K., ITOH, M., OOHASHI, H., ITAYA, Y., and YAMAMOTO, M.: '1.3-mm buried-heterostructure lasers using a CH_4 reactive-ion-etched mesa structure grown by metalorganic vapor phase epitaxy'. IPRM'96, Stadtgarten, Germany, April 1996, Paper TuB 2–3, pp. 384–387

Low-threshold room-temperature CW operation of ZnSe-based blue/green laser diodes grown on conductive ZnSe substrates

F. Nakanishi, H. Doi, N. Okuda, T. Matsuoka, K. Katayama, A. Saegusa, H. Matsubara, T. Yamada, T. Uemura, M. Irikura and S. Nishine

SCH laser structures of ZnCdSe/ZnSe/ZnMgSSe have been grown on conductive ZnSe substrates by molecular beam epitaxy. Continuous-wave laser operation at room temperature was observed at a wavelength of 527.9nm (2.349eV). The threshold current and threshold voltage were 44mA (222A/cm²) and 5.4V, respectively. A lifetime of 74s at a constant light output power of 2mW was obtained.

The first ZnSe-based blue-green laser diode (LD) was reported in 1991 [1] due to the success in p-type doping by active nitrogen [2]. Room-temperature continuous-wave (CW) operation was reported in 1993 [3], using wider bandgap ZnMgSSe cladding layers lattice-matched to GaAs, and in 1996 101.5h CW operation was realised [4]. To date, ZnSe-based LDs have mostly been prepared on GaAs substrates because of its close lattice matching (0.27%). However, due to both the hetero-valency and the differences in the thermal expansion coefficients between the GaAs substrate and the epitaxial layer, it is difficult to reduce the defect density generated at the hetero-interface to be as low as that of III-V LDs. Homo-epitaxial growth is one candidate for avoiding the problem with hetero-epitaxy and has the potential to extend the lifetime of the devices due to the slow rate of degradation [5]. In 1997, CW laser operation at room temperature by homo-epitaxy was reported [6], but the characteristics such as threshold current, threshold voltage and lifetime were not as good as expected, because semi-insulating ZnSe substrates were used. In this Letter, we report, for the first time, low threshold CW laser operation at room temperature, having a lifetime of > 1min at a constant light output power of 2mW, using conductive ZnSe substrates.

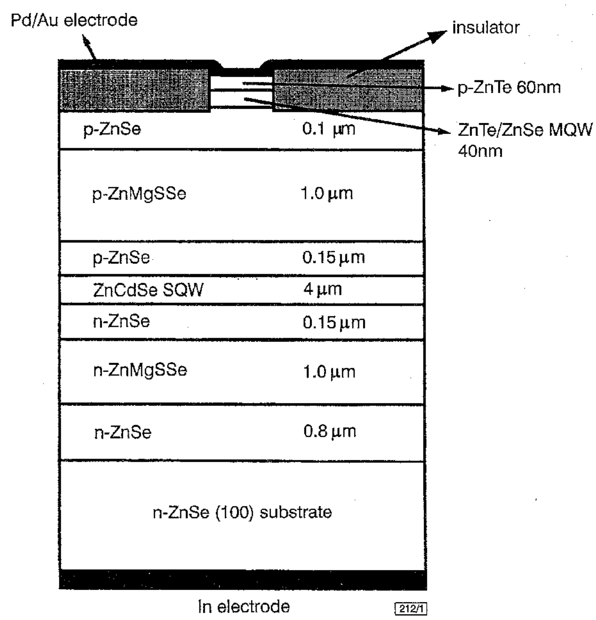

Fig. 1 *Schematic diagram of ZnCdSe/ZnSe/ZnMgSSe SCH laser diode on n-ZnSe substrate*

The laser diode structures were grown on n-type (100) ZnSe substrates by molecular beam epitaxy (MBE). ZnSe single crystals were also grown in our laboratories by the seeded chemical vapour transport method [7]. ZnSe wafers were cut from the ingot into substrates of ~ 1cm². The etch pit density (EPD) was $10^3 - 10^4 cm^{-2}$. The electron concentration of the substrate was $3 - 10 \times 10^{17} cm^{-3}$ at room temperature. After lapping and mechano-chemical polishing, the substrates were degreased using standard solvents, followed by a $K_2Cr_2O_7$:H_2SO_4:H_2O chemical etching process to remove the polishing damage. After that, the substrates were dipped into a diluted HF solution to reduce the ZnO layer at the surface. In the MBE growth chamber, ZnSe substrates were heated to a temperature of 300°C while being irradiated by active hydrogen from an RF plasma discharge source to remove the surface oxide layer. After plasma treatment, the reflection high energy electron diffraction (RHEED) pattern changed from a spotty 1 × 1 pattern to a streaky C (2 × 2) one.

Homo-epitaxial growth was carried out using solid sources, Se, Zn, Mg, ZnS, CdSe and Te. $ZnCl_2$ was used for n-type doping. The active nitrogen generated in the RF plasma discharge source was used for p-type doping. The growth temperature was ~ 300°C. The growth rate of each layer was 0.4–0.7µm/h. The schematic structure of the ZnCdSe/ZnSe/ZnMgSSe SCH laser is shown in Fig. 1. It consists of an *n*-ZnSe buffer layer ($n = 7 \times 10^{17} cm^{-3}$, d = 0.8µm); an *n*-ZnMgSSe cladding layer ($n = 5 \times 10^{17} cm^{-3}$, d = 1.0µm); an *n*-ZnSe optical guiding layer (d = 0.15µm); a ZnCdSe active layer (d = 4nm); a p-ZnSe optical guiding layer (d = 0.15 µm); a *p*-ZnMgSSe cladding layer (Na-Nd = $1 \times 10^{17} cm^{-3}$, d =